PROCEEDINGS OF THE ROYAL SOCIETY A

Proc. R. Soc. A (2005) **461**, 1735–1751
doi:10.1098/rspa.2005.1446
Published online 12 May 2005

Universal oscillations of high derivatives

By M. V. Berry

H.H. Wills Physics Laboratory, Tyndall Avenue, Bristol BS8 1TL, UK

Differentiation generates oscillations. For the nth derivative $f(n,t)$ of a function $f(t)$ that is analytic in a strip, including the real t-axis, the oscillations occupy a t interval that gets larger as n increases. The oscillations are studied in detail using integral representations and large-n asymptotics. For functions with singularities (poles or branch-points) in the complex t-plane, the oscillations of high derivatives are determined by the singularities; for entire functions, the oscillations originate in complex saddle-points. In a wide class of cases, the oscillations are contained in a Gaussian envelope in the t interval where $f(n,t)$ is largest, with the envelope including about $\sqrt{n}$ oscillations. Examples of the universal oscillations are given for $f(t)$ with a simple pole, competing branch-points, a single saddle, competing pole and saddle and where the zeros are confined to half the real axis.

Keywords: asymptotics; calculus; analysis

1. Introduction

My purpose is to explore a phenomenon associated with high derivatives of smooth functions $f(t)$ of a real variable t, that is

$$f(n,t) \equiv \frac{\mathrm{d}^n}{\mathrm{d}t^n} f(t), \tag{1.1}$$

for $n \gg 1$. High derivatives are of central importance in asymptotics (Dingle 1973), and indeed there is a sense in which differentiation is a primal operation in the generation of asymptotic series. This is because asymptotic series are based on local expansions (for example, of the exponent in an integrand about its saddle-points, or of the potential or refractive index in a wave equation about the point where the solution is sought). Therefore, successive orders of approximation involve successively higher derivatives, so the late terms of asymptotic series depend on high derivatives. High derivatives can also be regarded as iterates of the derivative map

$$f(t) \Rightarrow \frac{\mathrm{d}}{\mathrm{d}t} f(t).$$

The phenomenon, applicable to a wide class of functions including many that arise in mathematical physics, and surprising on first encounter, is as follows: for large n the local behaviour of $f(n,t)$ as a function of t is characterized by

Received 4 October 2004
Accepted 1 December 2004

trigonometric oscillations that get faster as n increases. For real $f(t)$, this can be loosely stated as follows: $\cos(\omega_n t+\gamma_n)$ (with ω_n increasing with n) is a universal attractor of the derivative map; the oscillations imply asymptotically equal spacing of the zeros of $f(n,t)$. For complex $f(t)$, the universal attractor is $\exp(\mathrm{i}\omega_n t)$, and the oscillations imply that as n increases the complex number $f(n,t)$ makes increasingly rapid circular windings round the origin $f=0$. (These attractors should be distinguished from the periodic orbits of the derivative map, which are combinations of exponential and trigonometric functions whose frequencies do not increase with n.)

These assertions seem surprising because differentiation is commonly regarded as a destabilizing operation, in contrast to integration which is a smoothing operation—yet here, under the operation of the differentiation map in reverse, that is, under successive integrations, the trigonometric oscillations diversify into all the different possible starting functions $f(t)$. But there is no paradox, since we shall see that the trigonometric oscillations are unstable in the sense of getting faster as n increases, and being multiplied by prefactors that increase factorially with n. The existence of the oscillations can be made immediately plausible by considering the Fourier transform $\bar{f}(\omega)$ of $f(t)$, which acquires a factor $(\mathrm{i}\omega)^n$ on differentiation, thereby suppressing low-frequency components and amplifying high-frequency ones.

As an elementary example introducing the universal oscillations, consider

$$f(t)=\frac{1}{(t-\mathrm{i})}, \tag{1.2}$$

for which

$$\begin{aligned} f(n,t) &= \frac{(-1)^n n!}{(t-\mathrm{i})^{n+1}} \\ &= -\frac{n!}{(t^2+1)^{(1/2)(n+1)}}\exp\left\{-\mathrm{i}(n+1)\left(\arctan t+\frac{1}{2}\pi\right)\right\}. \end{aligned} \tag{1.3}$$

Thus, the nth derivative is an oscillatory function of t, with $f(n,t)$ winding round the origin of the complex f-plane (figure 1) and $\mathrm{Re}\, f(n,t)$ possessing zeros (figure 2a). The zeros of $\mathrm{Re}\, f(n,t)$ lie in the interval $|t|\leq\cot[\pi/2(n+1)]\sim 2(n+1)/\pi$. This increases with n, so for sufficiently large n every t is in the oscillatory interval. The oscillation frequency and associated period T are

$$\omega(n,t)=\frac{2\pi}{T(n,t)}=\frac{\mathrm{d}}{\mathrm{d}t}(n+1)\arctan t=\frac{(n+1)}{1+t^2}, \tag{1.4}$$

implying faster oscillations of the higher derivatives near any t.

From equation (1.3), it follows that the curves traced by $f(n,t)$ in the complex f-plane as t increases are the sinusoidal spirals (figure 1) studied by Maclaurin three centuries ago (Lawrence 1972), whose representation in polar coordinates is

$$r(\phi)=n!\left[\cos\left(\frac{\phi}{n+1}\right)\right]^{n+1}\quad\left(-\frac{1}{2}\pi(n+1)<\phi<\frac{1}{2}\pi(n+1)\right). \tag{1.5}$$

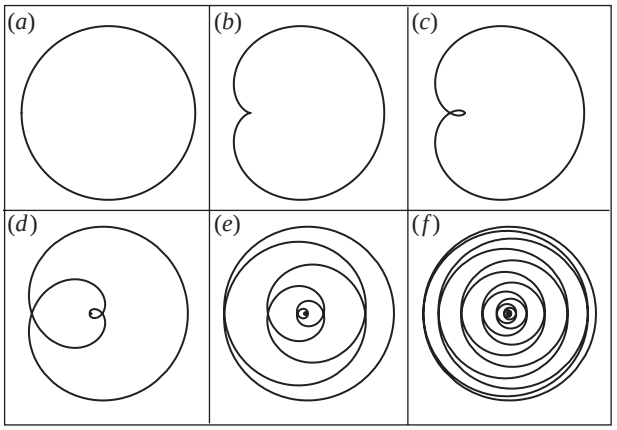

Figure 1. Derivatives of the function (1.2), with their oscillations represented by the spirals of equation (1.5) (rotated and scaled) traced by the complex function $f(n,t)$ as t increases, for (*a*) $n=0$, (*b*) $n=1$, (*c*) $n=2$, (*d*) $n=9$, (*e*) $n=50$ and (*f*) $n=200$.

The derivatives $f(n,t)$ are largest near $t=0$. In this region equation (1.3) can be approximated by

$$f(n,t) \approx -n!\exp\left\{-\frac{1}{2}(n+1)t^2\right\}\exp\left\{-\mathrm{i}(n+1)\left(t+\frac{1}{2}\pi\right)\right\} \quad (|t| \ll 1), \quad (1.6)$$

showing that where the derivatives are largest they can be represented by oscillatory Gaussians (figure 2*b*). The width of the Gaussians is $1/\sqrt{(n+1)}$, comfortably smaller than the range of validity of equation (1.6). The corresponding oscillation period is $t=2\pi/(n+1)$, so there are many oscillations (of order $\sqrt{n}$) within the Gaussian peak.

We will generalize this example to include functions $f(t)$ that are analytic in a strip including the real axis, and thus can be represented as contour integrals (§2). Determining the large-n behaviour of $f(n,t)$ is then an application of the asymptotics of integrals. The appropriate procedures depend on whether $f(t)$ has singularities in the finite t-plane (§2*a*) or is entire (§2*b*). In both cases, the large-n behaviour depends on the local behaviour of $f(t)$ at particular points in the complex plane. A variety of examples (§3*a*–*e*) illustrates the universality of the oscillation phenomenon.

High derivatives have been studied before in several contexts. As already mentioned, they are central in asymptotics. Dingle (1973) (especially §VII.2 and §VIII.1) gives several techniques for calculating the large-n behaviour of $f(n,t)$, though without drawing attention to the oscillations we are emphasizing. High derivatives arose naturally in the quantum evolution of slowly forced systems, as high-order iterates, under an adiabatic transformation, of the associated Hamiltonian operator. The universal oscillations were identified as a general phenomenon (Berry 1987) and described explicitly for complex functions with singularities (this result will be re-derived using a different method in §2*a*). There is a long history of studies of zeros of derivatives of entire functions, culminating in a recent paper by Farmer & Rhoades (2005; see also references therein), in which it is proved that for entire $f(t)$ the zeros of equation (1.1) become more

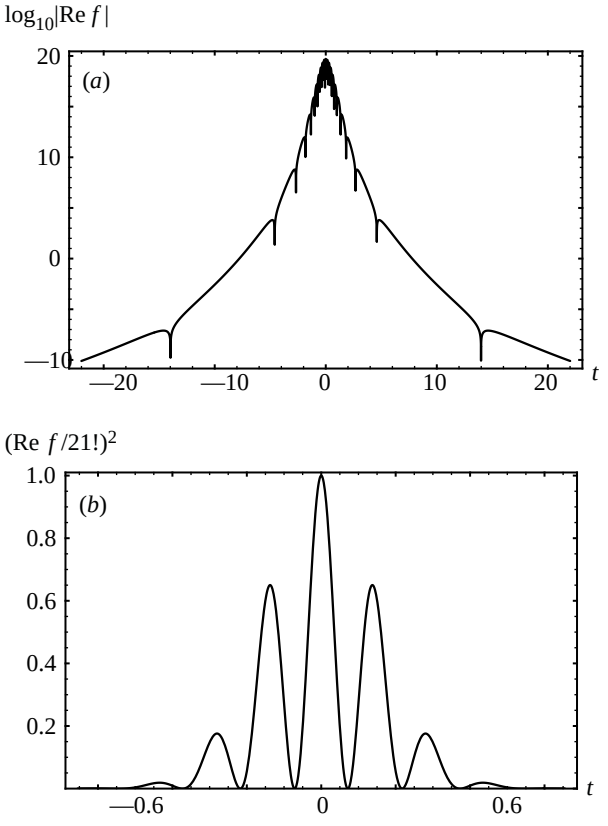

Figure 2. Universal oscillations of the twenty-first derivative of the function (1.2). (*a*) $\log_{10}|\mathrm{Re}\, f(21,t)|$: on this and later logarithmic plots the negative spikes correspond to zeros. The largest zeros lie at $t=\pm\cot(\pi/44)=13.98\ldots$. (*b*) Magnification of the region near the origin, plotted as $\mathrm{Re}^2\, f(21,t)$; this curve is indistinguishable from the Gaussian approximation in equation (1.6).

evenly spaced as n increases, with interesting applications to the zeros of derivatives of the characteristic polynomial of large real symmetric matrices, and the zeros of derivatives of the Riemann zeta function on the critical line.

2. General theory

Several different integral representations of the nth derivative in equation (1.1) will be convenient. The most general is the Cauchy integral

$$f(n,t)=\frac{n!}{2\pi\mathrm{i}}\oint_C \mathrm{d}z\,\frac{f(z)}{(z-t)^{n+1}}, \tag{2.1}$$

where C is a small loop surrounding the point $z=t$. With Cauchy's theorem, C can be expanded and deformed, at least until it encounters one or more singularities of $f(t)$. Such singularities determine the large-n behaviour of $f(n,t)$ (§2*a*), a phenomenon known as Darboux's theorem (Dingle 1973). If $f(t)$ has no

finite singularities, then the rapid variation of the factor $(z-t)^{n+1}$ implies that the integral is dominated by the saddle-points of its integrand (§2*b*).

(*a*) *Functions with pole or branch-point singularities*

A sufficiently general case is branch-points or poles at a complex point $t=a$, near each of which $f(t)$ has the form

$$f(t) \approx \frac{A}{(t-a)^{\mu}} \, (t \approx a \equiv a_1 + \mathrm{i}a_2). \tag{2.2}$$

We expand C in equation (2.1) to leave behind a loop C' surrounding a clockwise if μ is integer (i.e. a is a pole, as in equation (1.2), which corresponds to $\mu=1$), or surrounding the branch cut (chosen outwards) if μ is a non-integer (i.e. a is a branch-point). Then, the local behaviour of $f(n,t)$ is determined by approximating the integrand near a, i.e.

$$z = a + \zeta, \tag{2.3}$$

so that

$$\begin{aligned} f(n,t) &\approx \frac{An!}{2\pi\mathrm{i}(a-t)^{n+1}} \int_{C'} \frac{\mathrm{d}\zeta}{\zeta^{\mu}} \exp\left\{-\frac{(n+1)\zeta}{(a-t)}\right\} \approx \frac{A(-1)^n(n+\mu-1)!}{(t-a)^{n+\mu}(\mu-1)!} \\ &\equiv \frac{B_n}{(t-a)^{n+\mu}}. \end{aligned} \tag{2.4}$$

This well-known result, generalizing the example equation (1.3), can also be obtained by repeatedly differentiating just the singular part of equation (2.1) of $f(t)$, and can be regarded as the swelling of the range of validity of the local approximation (2.1) as n increases, to include more and more of the real axis.

Because of the factor involving $t-a$, $|f(n,t)|$ is largest close to $t=a_1$, which we refer to as points on the real axis directly 'below' a (if $a_2>0$, or 'above' a if $a_2<0$). Close to such points, equation (2.4) can be further approximated as

$$\begin{aligned} f(n,t) \approx \frac{B_n}{a_2^{n+\mu}} \exp\left\{-\frac{1}{2}\alpha^2(t-a_1)^2\right\} \exp\left\{-\mathrm{i}\omega(t-a_1) + \frac{1}{2}\mathrm{i}\pi(n+\mu)\right\} \\ (|t-a_1| \ll |a_2|), \end{aligned} \tag{2.5}$$

where

$$\alpha = \frac{\sqrt{n+\mu}}{a_2}, \quad \omega = \frac{(n+\mu)}{a_2}. \tag{2.6}$$

These results generalize equation (1.6).

The complex exponential in equation (2.5) displays the universal rapid oscillations, with local frequencies ω proportional to n. Therefore, the period of the oscillations is proportional to $1/n$, and since the Gaussian envelope has width $1/\sqrt{n}$ there are many (of order $\sqrt{n}$) oscillations in the region, below the singularity, where $f(n,t)$ is significant. Note that the oscillations get faster as a_2 gets smaller, that is, as the singularity approaches the real axis. We conclude

that on the part of the real axis close to a complex singularity, the high derivatives of functions are accurately represented by rapidly oscillating Gaussians.

For real functions $f(t)$, the singularities come in conjugate pairs, whose contributions add to give oscillations of the form $\cos(\omega(t-a_1))$. More generally, if there are several singularities, their leading-order large-n contributions, each of the form (2.4), add to give the asymptotic form of $f(n,t)$. For each t, the dominant oscillation comes from the singularity (or singularities) most nearly above or below t; the contributions from the others are exponentially smaller.

The factorial increase with n of the coefficient B_n in equation (2.4) underlies the divergence commonly encountered in asymptotic series, and, together with the increasingly fast oscillations (cf. equation (2.6)), reflects the instability of differentiation.

(*b*) *Entire functions: saddle-dominated derivatives*

If $f(t)$ has no finite singularities, it is convenient to define

$$f(t) \equiv \exp\{-g(t)\}, \tag{2.7}$$

so that equation (2.1) can be written

$$f(n,t) = \frac{n!}{2\pi \mathrm{i}} \oint_C \mathrm{d}z \, \exp\{-\Phi(z;n,t)\}, \tag{2.8}$$

where

$$\Phi(z;n,t) = (n+1)\log(z-t) + g(z). \tag{2.9}$$

Then the contour C can be expanded to pass through one or more of the saddles $z_m(n,t)$ of the exponent, defined by

$$\frac{\partial \Phi(z;n,t)}{\partial z} = 0 \Rightarrow (t - z_m(n,t))g'(z_m(n,t)) = (n+1). \tag{2.10}$$

Each will contribute to $f(n,t)$ according to the standard saddle-point method (Wong 1989), leading to

$$f(n,t) \approx \frac{n!}{\mathrm{i}\sqrt{2\pi}} \sum_m \frac{\exp\{-\Phi(z_m(n,t);n,t)\}}{\sqrt{g''(z_m(n,t)) - \frac{1}{(n+1)}\, g'(z_m(n,t))^2}}, \tag{2.11}$$

where the sum is over all saddles m that are accessible, in the sense that C can be locally deformed into a segment along the steepest-descent contour through $z_m(n,t)$. The oscillations are determined by the imaginary parts of the exponents Φ, and have frequencies ω and periods T given by

$$\omega(n,t) = \frac{2\pi}{T(n,t)} = \frac{\mathrm{d}}{\mathrm{d}t} \mathrm{Im}\, \Phi(z_m(n,t);n,t) = \frac{\partial}{\partial t} \mathrm{Im}\, \Phi(z_m(n,t);n,t)$$

$$= \mathrm{Im}\, g'(z_m(n,t)). \tag{2.12}$$

(For real $f(t)$, the asymptotic spacing of the zeros of $f(n,t)$ is $T(n,t)/2$.)

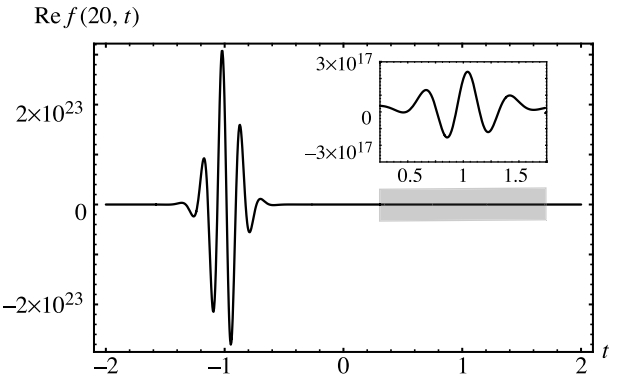

Figure 3. Competition between singularities, illustrated by Re $f(20, t)$ for the function (3.1) with two branch-points. The inset is a magnification of the shaded region by a factor $2^{20.5}=1.5\times10^6$. The curves, computed from the non-approximated $f(20, t)$, can hardly be distinguished from those (not shown) computed from the Gaussian approximation in equation (3.2).

The high derivatives of entire functions are complicated by the fact that the location of the contributing points $z_m(n,t)$ depends on n and t, rather than being constant as for functions with singularities. Several examples will be presented later.

3. Examples

(*a*) *Competing branch-points*

An example illustrating the additivity of contributions to high derivatives from competing singularities is

$$f(t) = \frac{1}{\sqrt{\left(t+1-\frac{1}{2}\mathrm{i}\right)(t-1-\mathrm{i})}}. \tag{3.1}$$

For large n, we can anticipate that $f(n, t)$ can be approximated as the superposition of two oscillatory Gaussians. Explicitly, from equation (2.5),

$$\begin{aligned} f(n,t) \approx & \frac{(-\mathrm{i})^n\left(n-\frac{1}{2}\right)!}{\sqrt{\left(\pi\left(2+\frac{1}{2}\mathrm{i}\right)\right)}}\exp\left\{\frac{1}{4}\mathrm{i}\pi\right\} \\ & \times\left[-\mathrm{i}2^{n+(1/2)}\exp\left\{-2\left(n+\frac{1}{2}\right)(t+1)^2\right\}\exp\left\{-2\mathrm{i}\left(n+\frac{1}{2}\right)(t+1)\right\}\right. \\ & \left.+\exp\left\{-\frac{1}{2}\left(n+\frac{1}{2}\right)(t-1)^2\right\}\exp\left\{-\mathrm{i}\left(n+\frac{1}{2}\right)(t-1)\right\}\right]. \end{aligned} \tag{3.2}$$

Since the branch-point above $t=-1$ is twice as close to the real axis as the branch-point above $t=+1$, the Gaussian near $t=-1$ is larger than that near $t=+1$ by a factor $2^{n+1/2}$, and has half the width and half the period. Figure 3

demonstrates the additivity of the two contributions: the Gaussian near $t=+1$ is clearly visible, even though it is a million times smaller than that near $t=-1$.

(*b*) *Gaussian*

A simple example of an entire function is

$$f(t)=\exp\left(-\frac{1}{2}t^2\right), \tag{3.3}$$

whose nth derivative is

$$f(n,t)=(-1)^n 2^{-n/2} H_n\left(\frac{1}{\sqrt{2}}t\right)\exp\left(-\frac{1}{2}t^2\right), \tag{3.4}$$

involving the Hermite polynomials. From the identities (Abramowitz & Stegun 1972)

$$\left.\begin{aligned}\lim_{n\to\infty}\frac{(-1)^n\sqrt{n}}{4^n n!}H_{2n}\left(\frac{x}{2\sqrt{n}}\right)&=\frac{1}{\sqrt{\pi}}\cos x,\\ \lim_{n\to\infty}\frac{(-1)^n}{4^n n!}H_{2n+1}\left(\frac{x}{2\sqrt{n}}\right)&=\frac{2}{\sqrt{\pi}}\sin x,\end{aligned}\right\} \tag{3.5}$$

follows

$$f(n,t)\approx n^{n/2}\exp\left(-\frac{1}{2}n\right)\sqrt{2}\cos\left(t\sqrt{n}+\frac{1}{2}n\pi\right)\quad(|t|\ll 1), \tag{3.6}$$

exhibiting the universal oscillations for small t, with period $T\sim 1/\sqrt{n}$.

A description of the oscillations with a wider range of validity than equation (3.6) can be found using known asymptotic formulae for Hermite polynomials. For later application, however, it is more convenient to use the saddle-point method of §2*b*. With $g(t)=t^2/2$, the condition (2.10) gives the two complex saddles

$$z_\pm=\pm\mathrm{i}\sqrt{n+1}\exp\left\{\mp\mathrm{i}\arcsin\frac{t}{2\sqrt{n+1}}\right\}\quad(|t|<2\sqrt{n+1}), \tag{3.7}$$

whence equation (2.11) gives

$$\begin{aligned}f(n,t)\approx&\frac{n^{n/2}\exp\left(-\frac{1}{2}n-\frac{1}{4}t^2\right)\sqrt{2}}{\left(1-\frac{t^2}{4(n+1)}\right)^{1/4}}\\ &\times\cos\left\{\frac{1}{2}t\sqrt{n+1-\frac{1}{4}t^2}+\left(n+\frac{1}{2}\right)\arcsin\frac{t}{2\sqrt{n+1}}+\frac{1}{2}n\pi\right\}\\ &(|t|<2\sqrt{n+1}).\end{aligned} \tag{3.8}$$

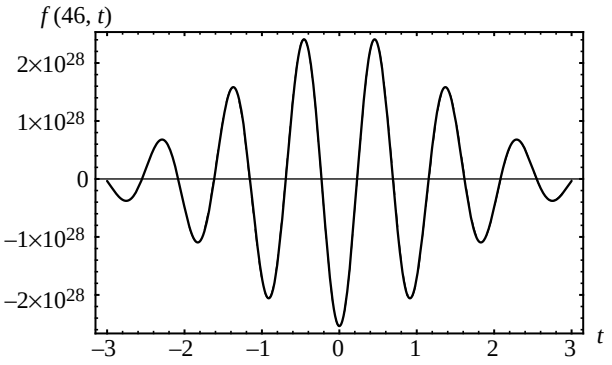

Figure 4. Universal oscillations in $f(46,t)$ for the Gaussian function (3.3); the curve is indistinguishable from the Gaussian approximation in equation (3.10).

The local oscillation frequency is from equation (2.12),

$$\omega(n,t) = \mathrm{Im}\, z_{\pm}(n,t) = \pm\sqrt{\left(n+1-\frac{1}{4}t^2\right)}, \tag{3.9}$$

showing that the oscillations get slower as t increases. Outside the oscillatory region $|t| > 2\sqrt{n+1}$ (which gets bigger with increasing n as expected for high derivatives), $f(n,t)$ decays rapidly and monotonically.

In fact, $f(n,t)$ gets rapidly smaller as $|t|$ increases even within the oscillatory region, as can be seen from the following approximation to equation (3.8), which is a slight refinement of equation (3.6)

$$f(n,t) \approx n^{n/2}\exp\left(-\frac{1}{2}n-\frac{1}{4}t^2\right)\sqrt{2}\cos\left(t\sqrt{n}+\frac{1}{2}n\pi\right) \quad (|t| \ll 2\sqrt{n+1}). \tag{3.10}$$

As with the singularities considered previously, there is a Gaussian envelope in the region of the t-axis near the contributing z points, in this case complex saddles close to $\pm\mathrm{i}\sqrt{n+1}$ (cf. (3.8) for small t). The width of the envelope is of order 1: much wider than the oscillation period, which is of order $1/\sqrt{n}$. This is illustrated in figure 4.

(*c*) *Saddle and pole*

For the function

$$f(t) = \frac{\exp\left(-\frac{1}{2}t^2\right)}{t-a}, \quad a = a_1 + \mathrm{i}a_2, \tag{3.11}$$

we can anticipate that the dominant contribution to $f(n,t)$ will come from the pole at $t=a$. However, associated with the Gaussian factor is a saddle-point of the integral (2.1), as described in §3(*a*), which will also contribute to the high derivatives. The saddle-point contribution is smaller (by a factor of order $n^{n/2}$) than that from the pole (of order $n! \sim n^n$). But the width of the saddle contribution in the region where it is significant is wider, and the period of its oscillations greater, than the corresponding contributions from the pole, both by a factor $\sqrt{n}$.

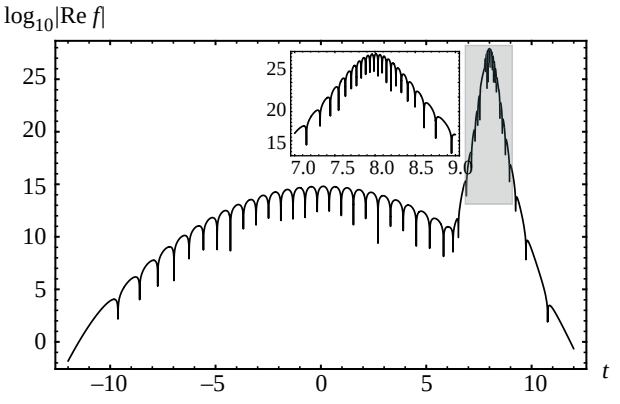

Figure 5. Competition between saddle and pole, illustrated by $\mathrm{Log}|\mathrm{Re}\, f(30,t)|$ for the function (3.11) with $a=8+\mathrm{i}/2$; the inset is a magnification of the shaded region.

Assuming additivity, we write the high derivatives of equation (3.11) as

$$f(n,t) \approx f_{\mathrm{pole}}(n,t) + f_{\mathrm{saddle}}(n,t). \tag{3.12}$$

The pole contribution is from equation (2.5)

$$\begin{aligned} f_{\mathrm{pole}}(n,t) &= -\frac{n!}{(a-t)^{n+1}}\exp\left(-\frac{1}{2}a^2\right) \\ &\approx -\frac{n!}{(\mathrm{i}a_2)^{n+1}}\exp\left\{-\frac{1}{2}\left[a^2+\frac{(n+1)}{a_2^2}(t-a_1)^2\right]\right\} \\ &\quad\times\exp\left\{-\mathrm{i}\frac{(n+1)}{a_2}(t-a_1)\right\} \quad (|t-a_1|\ll a_2). \end{aligned} \tag{3.13}$$

The contribution from the saddles, which for small t are close to $z_\pm=\pm\mathrm{i}\sqrt{(n+1)}$ (where the Gaussian contribution (3.10) is significant), and which dominates the factor $1/(z-a)$ in the integrand of (2.1), is

$$f_{\mathrm{saddle}}(n,t) \approx -n^{(1/2)(n-1)}\sqrt{2}\exp\left(-\frac{1}{2}n-\frac{1}{4}t^2\right)\sin\left(t\sqrt{n}-\frac{1}{2}n\pi\right). \tag{3.14}$$

To compare the two contributions, we define the ratio of their maxima

$$r(n,a) \equiv \frac{\left|f_{\mathrm{pole}}(n,a_1)\right|}{|f_{\mathrm{saddle}}(n,0)|} \approx \sqrt{2\pi}\,\frac{n^{(1/2)n+1}}{a_2^{n+1}}\exp\left(-\frac{1}{2}n\right), \tag{3.15}$$

showing how the pole dominates for sufficiently large n.

The oscillatory Gaussian contribution from the saddle is centred on $t=0$, and that from the pole is centred on $t=a_1$. To separate these contributions, we should choose a_1 non-zero. Figure 5 illustrates the faster oscillations and narrower Gaussian associated with the pole, superimposed on the oscillatory Gaussian associated with the saddle, for a case where the ratio $r(n,a)\sim 10^{13}$.

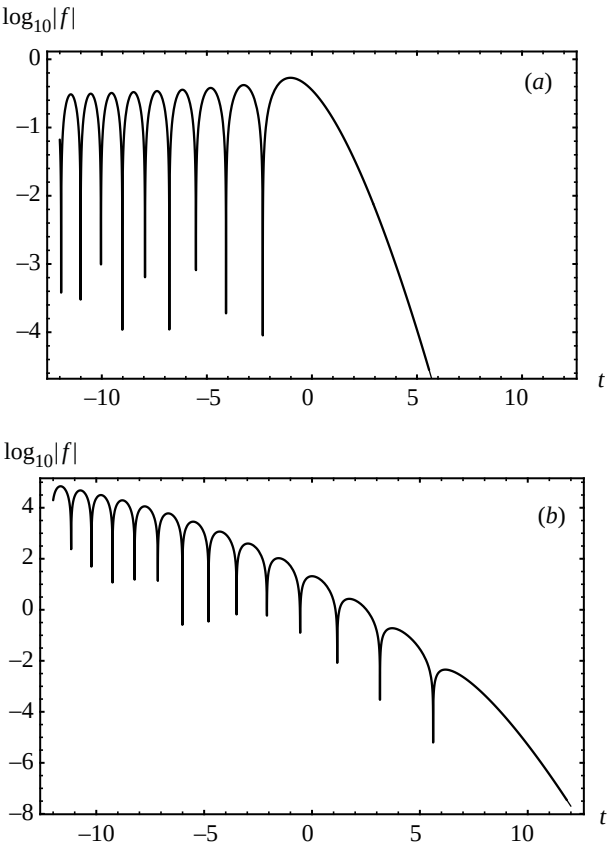

Figure 6. Logarithmic plots of (*a*) the Airy function and (*b*) its 10th derivative, showing migration of zeros onto the positive t-axis (in the region $t<10^{2/3}\tau_c=8.77\ldots$, where the zeros lie, this curve is indistinguishable from that computed using the approximation in equation (3.23)).

(*d*) *Airy function*

A very different type of entire function is the Airy function

$$f(t) = \mathrm{Ai}(t). \tag{3.16}$$

Even without differentiation, $\mathrm{Ai}(t)$ possesses infinitely many real zeros but these are confined to the negative t-axis (figure 6*a*). Elementary arguments indicate that increasing n will result in zeros migrating onto the positive t-axis, so that for sufficiently large n any t will lie in the oscillatory region of $f(n,t)$. This is illustrated in figure 6*b*, which was computed by expressing $f(n,t)$ as the sum of $\mathrm{Ai}(t)$ and its first derivative, each multiplied by a polynomial in t.

Rather than use the Cauchy integral (2.1) to understand the migration in detail, it is simplest to use the representation

$$\mathrm{Ai}(t) = \frac{\mathrm{i}}{2\pi}\int_C \mathrm{d}z\,\exp\left(-\frac{1}{3}z^3 + tz\right), \tag{3.17}$$

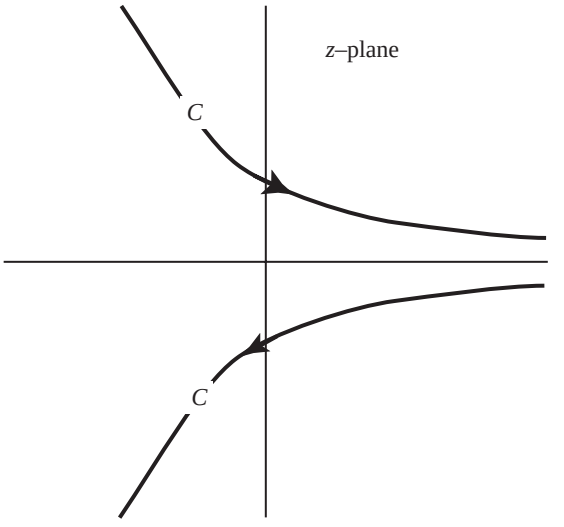

Figure 7. The integration contour for the Airy function. The asymptotes are $z=\infty$ and $z=\infty\exp(\pm 2\pi\mathrm{i}/3)$.

where C is the contour shown in figure 7. The convenient scaling

$$z = n^{1/3}\zeta, \quad t = n^{2/3}\tau, \tag{3.18}$$

then leads to

$$f(n,t) = \frac{\mathrm{i}}{2\pi}\, n^{n/3} \int_C \mathrm{d}\zeta\, \exp\left\{-n\Phi\left(\zeta, \frac{t}{n^{2/3}}\right)\right\}, \tag{3.19}$$

where

$$\Phi(\zeta,\tau) = \frac{1}{3}\zeta^3 - \tau\zeta - \log\zeta. \tag{3.20}$$

For large n, the integral will be dominated by its saddles, which satisfy

$$\zeta(\tau)^3 - \tau\zeta(\tau) - 1 = 0. \tag{3.21}$$

The oscillatory region—growing with n as expected—is $t<n^{2/3}\tau_{\mathrm{c}}$, where

$$\tau_{\mathrm{c}} = \frac{3}{2^{2/3}} = 1.88988\ldots. \tag{3.22}$$

Oscillations arise from the interference of contributions from two conjugate saddles $\zeta_{\pm}(\tau)$ (the third, real, saddle does not contribute), and the method of steepest descent leads to

$$f(n,t) \approx \sqrt{\frac{2}{\pi}}\, n^{(1/3)n-(1/6)} \exp\left(-\frac{1}{3}n\right) \mathrm{Im}\, \frac{\zeta_+(\tau)^{n+1}\exp\left\{\frac{2}{3}n\tau\zeta_+(\tau)\right\}}{\sqrt{2\zeta_+(\tau)^3+1}} \tag{3.23}$$

$(\tau<\tau_{\mathrm{c}})$.

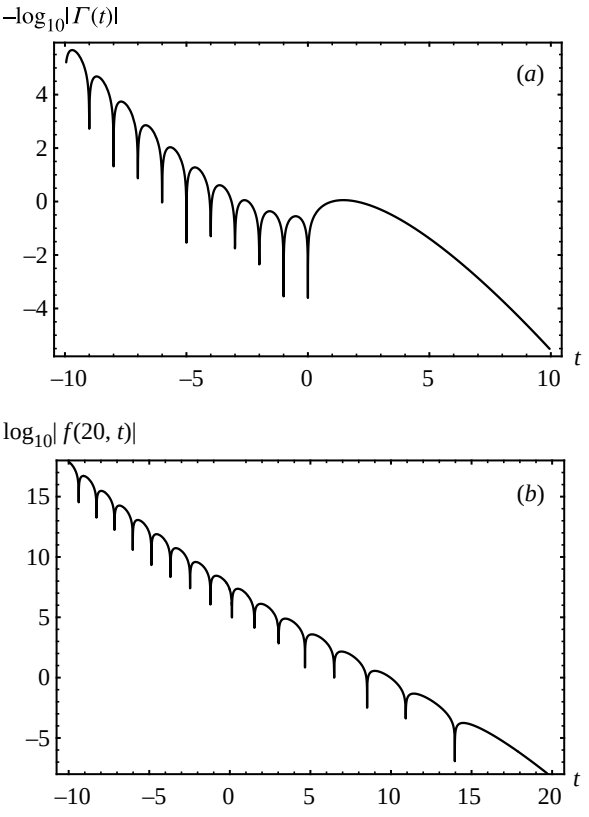

Figure 8. Logarithmic plots of (*a*) the reciprocal gamma function and (*b*) its 20th derivative, showing migration of zeros onto the positive t-axis, in the region $t<t_c(20)=17.16\ldots$. Where the zeros lie, this curve is almost indistinguishable from that computed using the approximation in equation (3.35).

The oscillations are fastest near $t=0$, and slow down near $t=n^{1/3}t_c$; their frequency is

$$\omega(n,t)=\frac{2\pi}{T(n,t)}=-n\,\mathrm{Im}\frac{\mathrm{d}\Phi(\zeta_+(\tau),\tau)}{\mathrm{d}t}=n^{1/3}\mathrm{Im}\;\zeta_+\left(\frac{t}{n^{2/3}}\right). \tag{3.24}$$

For the fastest oscillations, the saddle is

$$\zeta_+(0)=\exp\left(\frac{2}{3}\mathrm{i}\pi\right), \tag{3.25}$$

giving the frequency

$$\omega(n,0)=-\frac{\sqrt{3}}{2}n^{1/3},\quad T(n,0)=\frac{4\pi}{n^{1/3}\sqrt{3}}. \tag{3.26}$$

Again, we see the period T decreasing with n, in this case as $1/n^{1/3}$, as opposed to $1/n^{1/2}$ for the Gaussian (§3*b*) and $1/n$ for poles and branch-points (§2*a*).

(e) *Gamma function reciprocal*

Similar to the Airy function, but analytically more intricate, is

$$f(t) = \frac{1}{\Gamma(t)}, \tag{3.27}$$

which is an entire function with zeros at the negative integers (figure 8*a*). This example was suggested by Dr David Farmer. Again we expect zeros to migrate onto the positive t-axis as n increases, a process illustrated in figure 8*b*. This was computed by expressing $f(n,t)$ as a series involving polygamma functions (with the series for negative t evaluated using the reflection formula). The series is poorly conditioned so numerical evaluation is tricky and gives no insight into the behaviour of the zeros.

For analytical investigation, a convenient representation, valid for all t, is the Hankel integral

$$\frac{1}{\Gamma(t)} = \frac{\mathrm{i}}{2\pi}\int_C \mathrm{d}z(-z)^{-t}\exp(-z), \tag{3.28}$$

where

$$-z = z\exp(-\mathrm{i}\pi) \quad \text{and} \quad 0 < \arg z < 2\pi, \tag{3.29}$$

and C loops from $t=+\infty$ clockwise round the origin. Thus, the derivatives are

$$f(n,t) = \frac{\mathrm{i}}{2\pi}(-1)^n\int_C \mathrm{d}z\,\exp\{-\Phi(z;n,t)\}, \tag{3.30}$$

where

$$\Phi(z;n,t) = z + t\log(-z) - n\log\log(-z). \tag{3.31}$$

For large n, the integral is dominated by contributions from the two relevant saddle points $z_\pm(n;t)$, satisfying

$$\frac{\partial}{\partial z}\Phi(z;n,t) = 0 \Rightarrow \log(-z) = \frac{n}{z+t}. \tag{3.32}$$

The deportment of these saddles as t increases with n fixed is shown in figure 9: the saddles are complex conjugates, migrating negatively until, at some positive value $t_\mathrm{c}(n)$, they coalesce at a point $z_\mathrm{c}(n) = -|z_\mathrm{c}(n)|$ on the negative real axis and split into two real saddles. The coalescence satisfies not only equation (3.32) but also

$$\frac{\partial^2}{\partial z^2}\Phi(z;n,t) = 0 \Rightarrow \begin{cases} t_\mathrm{c}(n) = |z_\mathrm{c}(n)| + \dfrac{n}{\log|z_\mathrm{c}(n)|}, \\ |z_\mathrm{c}(n)|\log^2|z_\mathrm{c}(n)| = n, \end{cases} \tag{3.33}$$

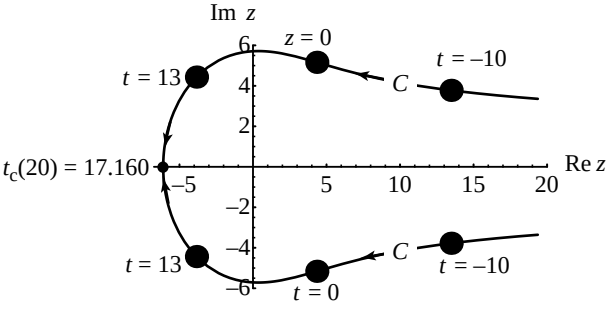

Figure 9. Migration of saddles in equation (3.32) of the integral (3.30) for reciprocal gamma derivatives, in the complex z-plane, for $n=20$, as t increases to $t_c(20)$.

so that

$$t_c(n) = \frac{n}{\log\{n/\log^2\{n/\log^2\{n/\ldots\}\}\}} + \frac{n}{\log^2\{n/\log^2\{n/\log^2\{n/\ldots\}\}\}}$$

$$\sim \frac{n}{\log n}. \tag{3.34}$$

The oscillatory region of $f(n,t)$ is $t<t_c(n)$; again this grows as n increases, to eventually include any fixed t. For $t>t_c(n)$, there are no zeros; $f(n,t)$ is dominated by the real saddle with the larger value of z, and decays rapidly.

Saddle-point integration now leads, for $t<t_c$, to

$$f(n,t) \approx (-1)^{n+1}\sqrt{\frac{2}{\pi|\Phi_{2+}|}}\exp(-\mathrm{Re}\,\Phi_+)\sin\left(\mathrm{Im}\,\Phi_+ + \frac{1}{2}\arg\Phi_{2+}\right), \tag{3.35}$$

where

$$\Phi_+ = \Phi(z_+(n,t);n,t), \quad \Phi_{2+} = \frac{\partial^2}{\partial z^2}\Phi(z_+(n,t);n,t). \tag{3.36}$$

For each n, the zeros $t_m(n)$ are given according to equation (3.35) by

$$\mathrm{Im}\,\Phi_+ + \frac{1}{2}\arg\Phi_{2+} = m\pi \quad (m=1,2,\ldots), \tag{3.37}$$

with $m=1$ corresponding to the largest zero (i.e. the zero closest to $t_c(n)$). The number $M(n)$ of zeros $t>0$ is therefore

$$M(n) = \mathrm{int}\left[\mathrm{Im}\,\Phi_+ + \frac{1}{2}\arg\Phi_{2+}\right]_{t=0} + 1. \tag{3.38}$$

This formula is illustrated in figure 10; it agrees perfectly with numerical computations based on the exact series for $f(n,t)$ (e.g. figure 8*a*,*b*). A rough approximation is

$$M(n) \sim \frac{n}{\log n}. \tag{3.39}$$

The general phenomenon of equalization of spacings between zeros by repeated differentiation can be illustrated near $t=0$. From equation (3.37),

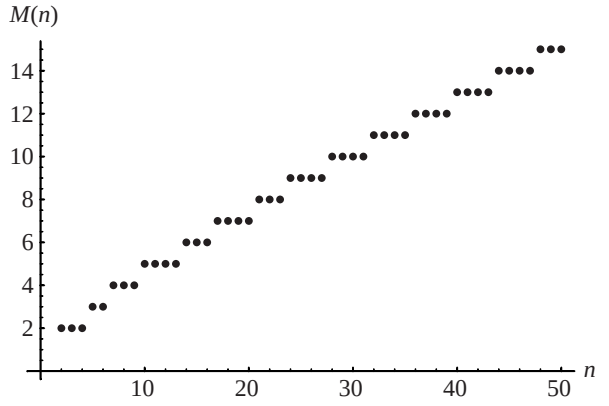

Figure 10. Number $M(n)$ of positive zeros of reciprocal gamma derivative, calculated from equation (3.38).

the period of $f(n,\ t{\sim}0)$ (twice the zero spacing) is

$$T(n,0) = \frac{2\pi}{(\partial\ \mathrm{Im}\ \Phi_+/\partial t)_{t=0}} = \frac{2}{1-(\arg z_+)_{(t=0)}/\pi}. \tag{3.40}$$

Some manipulation of the real and imaginary parts of equation (3.32), with $t{=}0$, shows that the spacing is $1/\gamma$, where γ is the solution of

$$\frac{\pi\gamma}{\sin(\pi\gamma)}\exp(-\pi\gamma\ \cot\ \pi\gamma) = n. \tag{3.41}$$

Asymptotically

$$\frac{1}{2}\,T(n,0) \sim 1 + \frac{1}{\log\ n}, \tag{3.42}$$

showing the equalization as $n{\to}\infty$.

The spacings increase with t, and the largest, near $t_{\mathrm{c}}(n)$, is

$$\frac{1}{2}\,T_{\max}(n) = t_1(n) - t_2(n), \tag{3.43}$$

A theory for $T_{\max}(n)$ can be constructed by expanding about $t_{\mathrm{c}}(n)$, noting the fact that $\mathrm{Im}\ \Phi_+$ vanishes as $(t_{\mathrm{c}}{-}t)^{3/2}$. For small m, this leads to

$$t_m(n) \approx t_{\mathrm{c}}(n) - \left(\frac{3}{2}\,\pi\left(m-\frac{1}{4}\right)\right)^{2/3} |z_{\mathrm{c}}(n)|\left|\frac{1}{2}\,\Phi_{3\mathrm{c}}(n)\right|^{1/3}, \tag{3.44}$$

where

$$\Phi_{3\mathrm{c}}(n) = \frac{\partial^3}{\partial z^3}\,\Phi(z_{\mathrm{c}}(n); n, t_{\mathrm{c}}(n)). \tag{3.45}$$

Thus, the largest spacing is, for large n,

$$\frac{1}{2}\,T_{\max}(n) \approx 1.399|t_{\mathrm{c}}(n)||\Phi_{3\mathrm{c}}(n)|^{1/3}. \tag{3.46}$$

A rough estimate is

$$\frac{1}{2}\,T_{\max}(n) \sim \left(\frac{n}{\log^2 n}\right)^{1/3}. \tag{3.47}$$

The saddle-point method fails at $t=t_{\mathrm{c}}(n)$ where the saddles coalesce and $\Phi_{2+}=0$. It is possible to derive an approximation that is uniformly valid through $t=t_{\mathrm{c}}(n)$ and for $t>t_{\mathrm{c}}(n)$, in terms of the Airy function $\mathrm{Ai}(x)$ and its derivative $\mathrm{Ai}'(x)$. However, since this is irrelevant to the zeros I do not give the formula here.

I thank Dr David Farmer for showing me a preprint of his paper with Rhoades, which stimulated me to write this one. My research is supported by the Royal Society of London.

References

Abramowitz, M. & Stegun, I. 1972 *Handbook of mathematical functions*. Washington, DC: National Bureau of Standards.

Berry, M. V. 1987 Quantum phase corrections from adiabatic iteration. *Proc. R. Soc. A* **414**, 31–46.

Dingle, R. B. 1973 *Asymptotic expansions: their derivation and interpretation*. Washington: Dover.

Farmer, D. W. & Rhoades, R. C. 2005 Differentiation evens out zero spacings. *Trans. Am. Math. Soc.* S0002-9947(05)03721-9.

Lawrence, J. D. 1972 *A catalog of special plane curves*. New York: Dover.

Wong, R. 1989 *Asymptotic approximations to integrals*. New York: Academic Press.